Development of electrical polarization at an antiferromagnetic transition in $FeVO_4$

2009 J. Phys.: Condens. Matter 21 456003

(http://iopscience.iop.org/0953-8984/21/45/456003)

J. Phys.: Condens. Matter **21** (2009) 456003 (5pp) doi:10.1088/0953-8984/21/45/456003

Development of electrical polarization at an antiferromagnetic transition in $FeVO_4$

A Dixit and G Lawes

Department of Physics and Astronomy, Wayne State University, Detroit, MI 48201, USA

E-mail: glawes@wayne.edu

Received 27 July 2009, in final form 30 September 2009
Published 21 October 2009
Online at stacks.iop.org/JPhysCM/21/456003

Abstract

We have probed changes in the magnetic, electrical, dielectric, optical, and thermodynamic properties of iron vanadate ($FeVO_4$) at two magnetic phase transitions. $FeVO_4$ exhibits two antiferromagnetic transitions at $T_{N1} = 22$ K and $T_{N2} = 15$ K. Below 15 K $FeVO_4$ develops an electric polarization, concomitant with the second antiferromagnetic transition and indicating strong magnetoelectric coupling. The powder averaged zero field electric polarization for the polycrystalline $FeVO_4$ sample is 6 μC m^{-2} and can be switched by reversing the poling voltage. The peaks for certain Raman modes at larger wavenumbers shift to slightly higher energies in the temperature range between T_{N1} and T_{N2}, but there is practically no change in the Raman spectra between the paramagnetic and ground states. These Raman features help to clarify the microscopic mechanisms for magnetoelectric coupling in $FeVO_4$.

(Some figures in this article are in colour only in the electronic version)

1. Introduction

There is considerable interest in understanding the fundamental properties of a new class of materials known as multiferroics, which exhibit the simultaneous presence of two or more ferroic order parameters [1, 2]. In this class of materials, magnetoelectric multiferroics exhibiting coupling between magnetic and ferroelectric order have been particularly widely studied. The large coupling between the magnetic and dielectric properties property of these materials may be exploited for novel device applications, including magnetic sensors, spintronics, and microwave communications [3–5]. Intrinsic multiferroicity, where ferroelectricity develops concurrently with magnetic ordering, has been observed in manganites [6], vanadates [7], and cuprates [8]. In these intrinsic multiferroics it is believed that the magnetic spin structure lowers the symmetry leading to a polar space group, which allows ferroelectric ordering. In order to develop tractable models for the physical mechanisms giving rise to multiferroic order, it is desirable to investigate systems having a single magnetic constituent. Among the various transition metal vanadates having the general formula $TM_3V_2O_8$, where TM is a magnetic transition metal (Cu, Ni, Co, or Mn) and V is non-magnetic, $Ni_3V_2O_8$ is the only member identified as an intrinsic multiferroic; the complex spin structure in $Ni_3V_2O_8$ producing ferroelectricity is believed to arise because of the two inequivalent Ni sites on this lattice [7].

While a number of other multiferroic materials having a single type of magnetic ion have been investigated previously, notably $MnWO_4$ [9] and $RbFe(MoO_4)_2$ [10], we have focused on iron vanadate because of the similarities between this system and multiferroic $Ni_3V_2O_8$. $FeVO_4$ is a triclinic system containing a chain structure built from Fe–O polyhedral, with the spin 5/2 Fe^{3+} ions having three distinct crystallographic sites separated by $(VO_4)^{3-}$ groups, containing non-magnetic V^{5+} ions [11]. This compound shows two distinct antiferromagnetic transitions at $T_{N1} \sim 22$ K and $T_{N2} \sim 15$ K [11]. Neutron studies on single crystal $FeVO_4$ [12] have found that the magnetic structure below $T_{N2} \sim 15$ K, is non-collinear and incommensurate, while between $T_{N1} \sim 22$ K and $T_{N2} \sim 15$ K, the magnetic structure is collinear and incommensurate. It has been suggested previously that these two magnetic transitions could indicate either decoupled magnetic systems or competing magnetic interactions [11]. Very recently it has been argued that $FeVO_4$ is an intrinsic multiferroic, with ferroelectric order developing below the spiral magnetic transition at $T_{N2} \sim 15$ K [12].

2. Experimental details

We synthesized polycrystalline iron vanadate ($FeVO_4$) powder samples starting from metal organic solutions. We prepared a homogeneous mixture of iron (II)-2 ethylhexanoate and

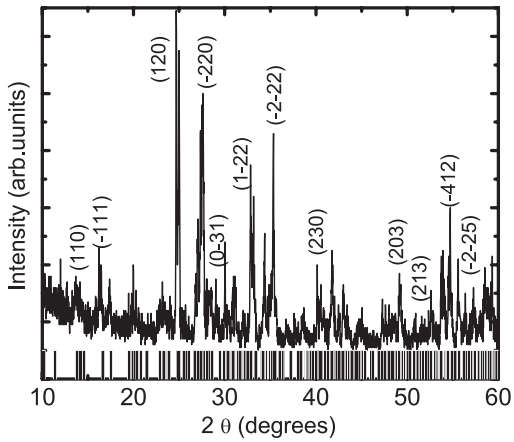

Figure 1. θ–2θ x-ray diffraction (XRD) pattern of the $FeVO_4$ powder sample. Although only certain reflections are given, all of the peaks can be fully indexed to $FeVO_4$. The expected peak positions are indicated by dashes along the lower edge of the figure.

vanadium naphthenate solutions having a Fe to V atomic ratio of 3:2. This specific stoichiometry was chosen for an unsuccessful attempt to synthesize $Fe_3V_2O_8$ as a structural analog of multiferroic $Ni_3V_2O_8$, but our synthesis using this atomic ratio unexpectedly produced single phase $FeVO_4$ iron vanadate. This homogeneous mixture was slowly heated to 350 °C for 2 h to burn off the organic constituents. The resulting black powder was sintered at 800 °C for 1 h in air, yielding a yellowish brown powder surprisingly identified as single phase $FeVO_4$. We note that a small amount of material spilled out of the crucible during the high temperature sintering step due to strong thermal agitation. We propose that this ejected material may have been Fe-rich, leading to only stoichiometric $FeVO_4$ remaining in the crucible.

We used a x-ray Rigaku RU2000 powder diffractometer to collect x-ray diffraction (XRD) patterns, which were used in the structural characterization of the sample. We measured room temperature Raman spectra on the $FeVO_4$ powder on a Triax Raman spectrometer using the 514.5 nm Ar-ion laser line. We measured the temperature dependent magnetization using the ac susceptibility option on a Quantum Design physical property measurement system (PPMS). For the heat capacity measurements, we mixed the $FeVO_4$ sample with Ag powder in a 1:1 ratio, then cold-pressed the composite into a solid pellet to ensure good internal thermal contact. The heat capacity was measured using the standard relaxation technique on a Quantum Design PPMS, and the contribution from the silver powder was measured separately and subtracted. We measured the dielectric constant and pyrocurrent with an Agilent 4284A Precision LCR meter and a Keithley 6517A high resistance electrometer respectively, on a pressed pellet of $FeVO_4$ sample in a parallel plate geometry having electrodes fashioned from silver epoxy.

3. Result and discussions

The XRD pattern on the $FeVO_4$ powder is shown in figure 1. The peaks from this polycrystalline sample can be completely

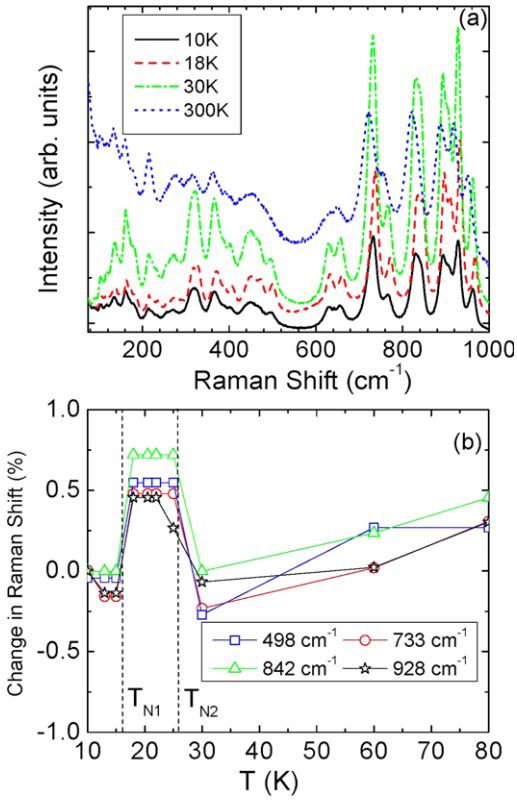

Figure 2. (a) Raman spectra on $FeVO_4$ bulk powder sample measured at different temperatures. (b) Relative change (in %) of the Raman shift for the 498, 733, 842 and 928 cm^{-1} modes with temperature.

matched to the reported XRD pattern for $FeVO_4$ (JCPDS # 38-1372). We have labeled some of the peaks in this XRD pattern. Rather unexpectedly, despite the excess Fe included in the precursor solution, we do not see any additional XRD peaks that could be associated with secondary phases; there is no evidence for iron oxide impurity phases in this sample. Although these XRD studies cannot not rule out the possibility of amorphous impurity phases, our Raman, magnetic, and heat capacity measurements, discussed in the following, are also all consistent with single phase $FeVO_4$. The iron vanadate ($FeVO_4$) crystal structure is triclinic system having the space group $P\bar{1}$, which is the only stable phase at ambient condition [11].

To further probe the lattice structure of the $FeVO_4$ sample, we have also conducted room temperature Raman measurements. We plot Raman spectra for $FeVO_4$ in figure 2(a) at different temperatures. The room temperature data are in good agreement with a previously measured Raman spectrum on this system [13]. The unit cell for $FeVO_4$ contains of a total of 36 atoms consisting of three symmetry-inequivalent VO_4 tetrahedra, two symmetry-inequivalent FeO_6 octahedra, and one FeO_5 polyhedron [14]. The point group for $FeVO_4$ is C_i, leading to 54 Raman active optical modes belonging to the A_g irreducible representation, with the remaining 51 IR active optical modes belong to A_u. We observe a total of 29 Raman active modes in the spectra shown in figure 2(a). The temperature dependence of these Raman

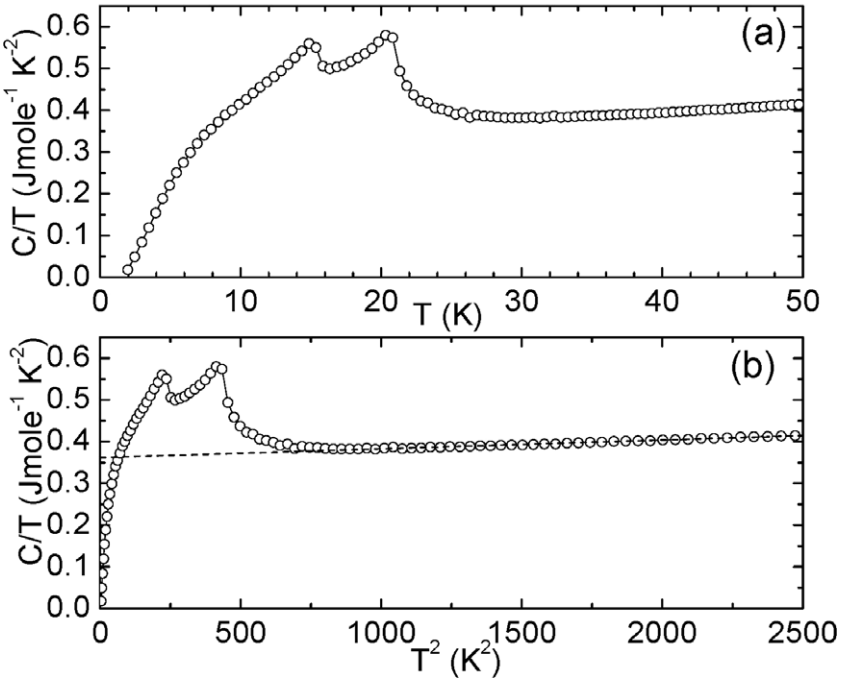

Figure 3. Temperature dependence of the heat capacity for $FeVO_4$ powder sample at zero magnetic field plotted as: (a) C/T versus T and (b) C/T versus T^2. The dashed line in panel (b) gives the best fit at higher temperatures to $C(T) = \gamma T + \alpha T^3$.

modes serves to divide them into two categories. The first set of Raman modes do not show any significant temperature dependence, beyond some small uniform softening on cooling, and typically fall at smaller Raman shifts. These modes occur at 104, 119, 214, 253, 270, 404, 449, and 473 cm^{-1} and can be associated with bending modes and with vibrations of FeO_x polyhedra [14].

The second class of modes shows systematic changes in the Raman shift in the temperature region between T_{N1} and T_{N2}, corresponding to the collinear antiferromagnetic phase. These modes fall at larger Raman shifts and are associated with the stretching of V–O–Fe and Fe–O bonds and the bending of Fe–O–V and Fe–O–Fe complexes [14]. The relative change in representative Raman modes at 498, 733, 842 and 928 cm^{-1} with temperature is plotted in figure 2(b). This second category of modes shows an abrupt relative increase of approximately 0.5% in Raman shift in the temperature interval between T_{N1} and T_{N2}. At low temperatures (below T_{N2}) and at high temperature (above T_{N1}) the peak positions for these modes are very similar. This suggests that the mechanism producing the shift in the higher energy Raman modes is only relevant in the collinear incommensurate magnetic phase. One possibility is that exchange striction in the collinear phase can change the phonon frequencies by modifying the effective elastic constant leading to a slight increase in the Raman shifts. Such a shift in the optical phonon modes associated with long range magnetic order has been proposed previously in the context of magnetically induced changes in the low frequency dielectric constant [15]. In this scenario, the polar displacements associated with the development of ferroelectricity would eliminate this magnetic exchange produced shift, in turn reducing the phonon mode frequencies to their original values. The fact that the Raman spectra are the same in the low temperature and high temperature phases suggests that the development of this polar phase does not significantly change the normal vibrations in the system despite the very small shifts in ion position that accompany a finite ferroelectric moment.

The temperature dependence of the specific heat capacity for the $FeVO_4$ powder sample is shown in figures 3(a) and (b). These data have been corrected for the contributions from the silver powder. The heat capacity shows two clear lambda-type anomalies around 15.4 and 21.7 K, corresponding to the two magnetic phase transitions in this system. As has been observed previously [11, 12], considerable magnetic entropy is removed well above these long range ordering transitions due to the development of short range magnetic correlations. The heat capacity in the intermediate temperature range between approximately $T = 30$ and 50 K can formally be fit to $C = \gamma T + \beta T^3$, with $\gamma = 0.35$ J mol^{-1} K^{-1} and $\beta = 2.2 \times 10^{-5}$ J mol^{-1} K^{-4}, as shown in figure 3(b). These values differ slightly from those obtained on single crystal $FeVO_4$ extracted over the same high temperature range [12]. Although this T^3 term in the heat capacity almost certainly includes contributions from both lattice and magnetic components, we can formally extract an effective Debye temperature from β, which gives $\theta_{D,eff} = 810$ K. This is close to the value of $\theta_{D,eff} = 773$ K extracted for single crystal samples over these higher temperatures [11], but much larger than the $\theta_D = 385$ K used to estimate the lattice contribution to specific heat in polycrystalline $FeVO_4$ samples [12]. This confirms the suggestion that there may be magnetic contributions to the higher temperature T^3 heat capacity term. There is also evidence for magnetic contributions to the linear term in the heat capacity. This linear contribution, γT, is often

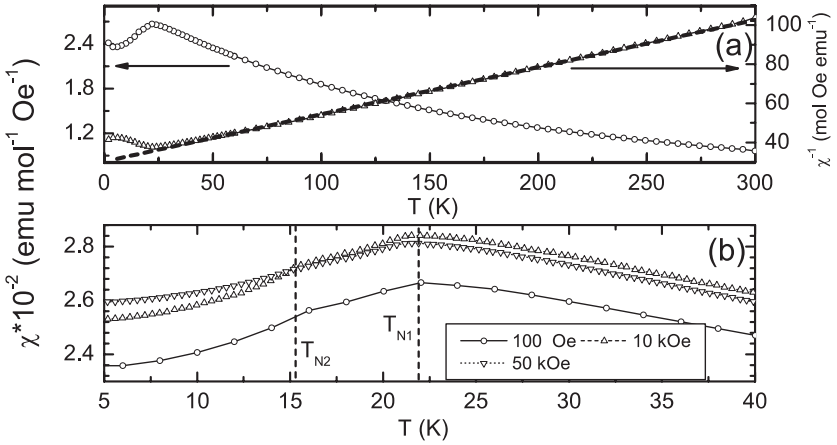

Figure 4. (a) Temperature dependence of the magnetic susceptibility and inverse magnetic susceptibility for $FeVO_4$ powder measured at 100 Oe. The dashed line shows the high temperature Curie–Weiss fit described in the text. (b) Magnetic susceptibility at $H = 100$ Oe, 10 and 50 kOe.

associated with charge carriers and would normally not be expected for insulating samples. However, such linear heat capacity terms have been observed previously in insulating magnets and attributed to spin-glass- or cluster-glass-like fluctuations [16]. At present, the origins of linear and cubic magnetic contributions to the heat capacity of $FeVO_4$ above the ordering temperature remain unclear, but may point towards the development of strong correlations in the paramagnetic phase.

We plot the temperature dependent magnetic susceptibility measured at a field of 100 Oe in figure 4(a). We also plot the temperature dependence of the inverse susceptibility in this same figure. We observe a peak in the susceptibility close to 22 K, corresponding to the onset of the higher temperature incommensurate magnetic order, and a small change of slope close to 15 K, associated with the development of the lower temperature incommensurate order. We fit the high temperature inverse susceptibility to the Curie–Weiss equation, $\chi = C/(T - \Theta_{CW})$, where χ is magnetic susceptibility, C the Curie–Weiss constant and Θ_{CW} is the Curie–Weiss temperature. We found that the Curie–Weiss constant C and Curie–Weiss temperature Θ_{CW} are 4.15 emu K mol^{-1} and -126 K respectively. The effective moment in the paramagnetic phase, calculated from the Curie constant C, is $\sim$5.54 μ_B. This value is close to the $\mu_{eff} = 5.92$ μ_B expected for $S = 5/2$ Fe^{3+} ions. The Curie–Weiss constant, $\Theta_{CW} = -126$ K, is large compared to the ordering temperature, consistent with the observation of considerable magnetic entropy above T_N. Figure 4(b) shows the susceptibility measured at $H = 100$ Oe, 10 and 50 kOe close to the transition. The susceptibility measured at 100 Oe is slightly smaller than that measured at higher fields, which may tentatively be attributed to a small offset from trapped flux in the superconducting magnet, which can be on the order of several Oe. The low field data more clearly show the two distinct magnetic transitions at $T_{N1} = 21.7$ K and $T_{N2} = 15.4$ K. These transitions shift almost negligibly even with an applied field of $H = 50$ kOe. This is consistent with the strong magnetic interactions inferred from the large Curie–Weiss temperature.

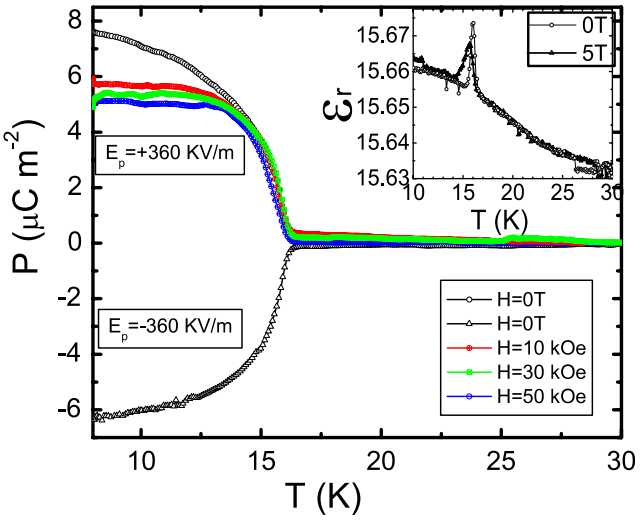

Figure 5. Polarization for $FeVO_4$ powder sample measured at poling fields $E = \pm 360$ kV m^{-1} under zero magnetic field, and for $E = +360$ kV m^{-1} with magnetic fields of $H = 10$, 30 and 50 kOe. Inset: temperature dependence of dielectric constant measured at $H = 0$ and 50 kOe.

The most significant characteristic of $FeVO_4$ is the development of an electrical polarization, associated with ferroelectric order [12], coincident with the lower temperature phase transition. In order to probe the development of this polarization, we have measured the temperature dependent dielectric constant, as shown in the inset to figure 5. The magnitude of the dielectric constant we obtain, roughly 15.5, is slightly smaller than the value of 18 obtained on other $FeVO_4$ powder samples [12]. The loss is on the order of $\tan\delta < 0.001$, consistent with $FeVO_4$ being a good dielectric. The dielectric constant shows a sharp peak at $T_{N2} = 15.4$ K, associated with the divergence of the electric susceptibility at the ferroelectric transition. The dielectric anomaly corresponds to a change of roughly 0.1% in the dielectric constant. This is

much smaller than typically observed in single crystal samples, for example the 18% change in single crystal $Ni_3V_2O_8$ [17], but is consistent with the size of the anomalies measured in polycrystalline samples, for example the 0.2% change in powder $Ni_3V_2O_8$ [17]. This anomaly shifts slightly in an applied magnetic field, by approximately $\Delta T_{N2} = 0.5$ K in a field of $H = 50$ kOe. There is no dielectric anomaly associated with the onset of magnetic order at T_{N1}, suggesting that the intrinsic magnetodielectric coupling in this material may be relatively small. We determined the spontaneous polarization of $FeVO_4$ in the polar phase by integrating the pyrocurrent measured on warming at zero bias. The polarization is shown in figure 5, poled with both positive ($+358$ kV m^{-1}) and negative (-358 kV m^{-1}) fields at $H = 0$. The polarization for this powder sample is ~ 6 μC m^{-2}, which is consistent with previous measurements [12]. We note that the measured pyrocurrent arises from the powder average of the polarization vector. Since the spontaneous polarization in intrinsic multiferroics is typically highly anisotropic [7, 18], we expect that the intrinsic polarization for $FeVO_4$ is much larger than our measured value. Assuming that the polarization is oriented along a single direction and that we are measuring the powder averaged projection of the signal along this direction, we find that the intrinsic polarization in $FeVO_4$ could be as large as 40 μC m^{-2}. This is somewhat smaller than the polarization of roughly 150 μC m^{-2} measured in multiferroic $Ni_3V_2O_8$, but very consistent with many other magnetically induced ferroelectrics. We have also measured the polarization for our powder sample under applied magnetic fields. In addition to the slight shift in transition temperature also seen in the dielectric measurements, we find that the magnitude of the polarization is slightly suppressed in an applied field, decreasing by approximately 17% in a field of $H = 50$ kOe.

4. Conclusion

We find that $FeVO_4$ exhibits a finite electrical polarization in the spiral incommensurate magnetic phase, consistent with previous reports [12]. The spontaneous polarization in our polycrystalline samples is relatively small, only 6 μC m^{-2}, but if we assume that this value represents the powder average of the uniaxial polarization normally developing in spin-spiral multiferroics, the intrinsic polarization in $FeVO_4$ could be as large as 40 μC m^{-2}. There is thermodynamic evidence for strong correlations developing above the antiferromagnetic ordering temperature, indicative of frustrated magnetic interactions. Most significantly, we find that specific Raman modes associated with Fe–O–V vibrations, show a distinct shift towards slightly higher (0.5%) energies in the collinear incommensurate magnetic phase, but that the Raman spectra in the paramagnetic and multiferroic phases are practically identical. This result points to the importance of spin–lattice coupling in determining the properties of $FeVO_4$, and that this coupling can produce significant changes in the non-polar phases.

Acknowledgments

This work was supported by the NSF through DMR-0644823. We acknowledge helpful conversations with C Sudakar and R Naik.

References

[1] Eerenstein W, Mathur N D and Scott J F 2006 *Nature* **442** 759
[2] Hill N A 2000 *J. Phys. Chem.* B **104** 6694
[3] Yang C H, Koo T Y and Jeong Y H 2005 *Solid State Commun.* **134** 299
[4] Haris A B and Lawes G 2007 *The Handbook of Magnetism and Advanced Magnetic Materials* (London: Wiley)
[5] de Sousa R and Moore J E 2008 *J. Nanoelectron. Optoelectron.* **3** 77
[6] Kimura T, Goto T, Shintani H, Ishizaka K, Arima T and Tokura Y 2003 *Nature* **426** 55
[7] Lawes G, Harris A B, Kimura T, Rogado N, Cava R J, Aharony A, Entin-Wohlman O, Yildirim T, Kenzelmann M, Broholm C and Ramirez A P 2005 *Phys. Rev. Lett.* **95** 087205
[8] Kimura T, Sekio Y, Nakamura H, Siegrist T and Ramirez A P 2008 *Nat. Mater.* **7** 291
[9] Arkenbout A H, Palstra T T M, Siegrist T and Kimura T 2006 *Phys. Rev.* B **74** 184431
[10] Kenzelmann M, Lawes G, Harris A B, Gasparovic G, Broholm C, Ramirez A P, Jorge G A, Jaime M, Park S, Huang Q, Shapiro A Ya and Demianets L A 2007 *Phys. Rev. Lett.* **98** 267205
[11] He Z, Yamaura J and Ueda Y 2008 *J. Solid State Chem.* **181** 2346
[12] Daoud-Aladine A, Kundys B, Martin C, Radaelli P G, Brown P J, Simon C and Chapon L J 2008 arXiv:0812.4429V1
[13] Tian H, Wachs I E and Briand L E 2005 *J. Phys. Chem.* B **109** 23491
[14] Brazdova V, Ganduglia-Pirovano M V and Sauer J 2005 *J. Phys. Chem.* B **109** 394
[15] Lawes G, Ramirez A P, Varma C M and Subramanian M A 2003 *Phys. Rev. Lett.* **91** 257208
[16] Ghivelder L *et al* 1999 *Phys. Rev.* B **60** 12184
[17] Kharel P, Kumarasiri A, Dixit A, Rogado N, Cava R J and Lawes G 2009 *Phil. Mag.* **89** 1923
[18] Goto T, Kimura T, Lawes G, Ramirez A P and Tokura Y 2004 *Phys. Rev. Lett.* **92** 257201